Measuring and modeling twilight's purple light

Raymond L. Lee, Jr. and Javier Hernández-Andrés

During many clear twilights, much of the solar sky is dominated by pastel purples. This purple light's red component has long been ascribed to transmission through and scattering by stratospheric dust and other aerosols. Clearly the vivid purples of post-volcanic twilights are related to increased stratospheric aerosol loading. Yet our time-series measurements of purple-light spectra, combined with radiative transfer modeling and satellite soundings, indicate that background stratospheric aerosols by themselves do not redden sunlight enough to cause the purple light's reds. Furthermore, scattering and extinction in both the troposphere and the stratosphere are needed to explain most purple lights. © 2003 Optical Society of America

OCIS codes: 010.1290, 330.1710, 330.1730.

1. Introduction

Ever since the Krakatoa volcano's explosion in August 1883, major volcanic eruptions have been followed by reports worldwide of extraordinarily vivid, often purplish, skies during clear twilights. Here we call this characteristic feature of the solar sky during post-eruption twilights the *volcanic purple light*. Naturally, volcanic purple lights occurred long before the Krakatoa eruption, and scattered accounts of these date from at least the early 16th century.[1]

After the Krakatoa event, 19th-century scientists quite reasonably speculated that the eruption injected dust into the upper atmosphere and that the twilight Sun's light was scattered by the resulting dust layers (or cloud droplets with dust nuclei) to form the purple light.[2,3] Some early authors assumed that spectrally selective diffraction by these relatively large scatterers caused the phenomenon's red component,[3,4] whereas others viewed the scatterers primarily as a means for scattering already reddened sunlight toward the surface.[5] Not surprisingly, still other writers favored a combination of diffraction and single scattering.[6]

Thus began the long and close association of the volcanic purple light with stratospheric dust and ash.[7–11] Yet even during volcanically quiet periods, pastel purples often dominate the solar sky during clear twilights, and stratospheric dust has been used to explain this *ordinary purple light* too.[12–14] Although some authors have been cautious about identifying these stratospheric scatterers as dust,[5,15] only fairly recently have twilight colors been linked definitively (but not exclusively) to scattering by sulfuric acid droplets in the stratosphere.[16,17]

2. Phenomenology of the Purple Light

Whatever the choice of scatterers, all existing purple-light models emphasize the role of the stratosphere, not the troposphere. Even authors who clearly note the troposphere's role in reddening sunlight tend not to dwell on it, instead understandably focusing their attention on the geometry of scattering in the stratosphere.[5,14] One of the few exceptions is Deirmendjian, who wrote in 1973 about the "close dependence of twilight features on the optical characteristics of the local and trans-horizon troposphere, and their variation not only along the vertical but along the horizontal direction as well, and . . . the highly subjective nature of individual impressions of twilight colors, relative brightness, and their changes with time."[10]

Indeed, our measurements and modeling of scores of clear twilights indicate that *both* the troposphere and stratosphere are crucial to explaining the formation and the absence of the ordinary purple light. Furthermore, the subjectivity that Deirmendjian notes necessarily pervades existing qualitative descriptions of the purple light. This subjectivity has

R. L. Lee, Jr. (raylee@usna.edu) is with the Mathematics and Science Division, U.S. Naval Academy, Annapolis, Maryland 21402. J. Hernández-Andrés is with the Departamento de Óptica, Facultad de Ciencias, Universidad de Granada, Granada 18071, Spain.

Received 18 January 2002; revised manuscript received 13 May 2002.

0003-6935/03/030445-13$15.00/0

© 2003 Optical Society of America

made purple-light phenomenology fairly imprecise to date, and this imprecision leads to confusion about which purple-light features are common and which are not. A corollary problem is that existing descriptions fail to mention some purple-light phenomena that we observed often during our research.

For example, Neuberger's diagram and description of evening purple light indicate that it begins as a small circle, approximately 10°–15° in diameter above the Sun's azimuth.[12] Minnaert makes this spot's initial view-elevation angle $h \sim 25°$ above the astronomical horizon[14]; apparently this is the "purple spot" variant mentioned by Gruner and Kleinert.[5] However, Minnaert soon dismisses this "purple patch" as the least common of five ways in which the purple light starts. His preferred origins include an outgrowth of the antitwilight arch that "spreads *more or less invisibly* over the zenith and on reaching the west becomes visible there" (emphasis added).[14] Bafflement is an understandable reaction to such conflicting (and sometimes invisible) visual descriptions. In fact, only once during our research did we see any feature that could be described as a "purple patch." It occurred well after the onset of evening purple light, changed shape and position rapidly, and clearly was caused by low-contrast crepuscular rays rotating across the sky (this rotation is most easily seen in time-lapse photography).

Adding to the purple light's phenomenological confusion is the older practice of using "intensity" as a synonym for "colorimetric purity." Thus, when Neuberger and Minnaert refer to its maximum *intensity* occurring at unrefracted solar elevation $h_0 \sim -4°$, they actually mean that its *purity* is greatest then.[12,14] In fact, both the radiance and luminance of skylight decrease nearly logarithmically during evening twilight. However, quite early in our research one of us (Lee) succumbed to this long-standing confusion about intensity versus purity by replacing "intensity" with "luminance" rather than "purity" when he revised Neuberger's purple-light entry in a meteorological dictionary.[18]

We describe the evolution and shape of the purple light more prosaically: It becomes visible imperceptibly, and its commonest form is a broad, vaguely eyelid-shaped region centered on the Sun's azimuth (although attempting to assign the purple light any shape is problematic). Figure 1 shows the typical color range, although not the full angular extent, of an ordinary purple light. Contrary to existing descriptions that restrict the purple light to an azimuthal width of 40°–80° and a maximum height of ~45°, we sometimes observe the entire twilight sky to be purplish (Fig. 2). We routinely estimate the purple light's maximum width as 90°–150°, and we can find its characteristic colorimetric signature at the zenith. Equally significant in our research is the fact that the purple light exhibits great diurnal variability, sometimes failing to appear at all (Fig. 3). Time-lapse photography graphically demonstrates one feature that our predecessors commented on, the dramatic setting and disappearance of the purple light as evening civil twilight ends.

Fig. 1. Photograph of an ordinary purple light taken during evening twilight at Chesapeake Beach, Maryland, on 23 February 1997 at 2250 UTC. Unrefracted solar elevation, $h_0 = -0.39°$; azimuth relative to the Sun, $\phi_{rel} = 0°$ at image center.

3. Canonical Purple-Light Geometry, Colorimetry, and Photometry

To quantify purple-light colors, from 1998 to 2001 we made time-series measurements of ~100 clear twilights' spectra at four sites: (1) Owings, Maryland, (2) the U.S. Naval Academy (USNA) in Annapolis, Maryland, (3) Spain's University of Granada, and (4) a rural site near Marion Center, Pennsylvania.[19] All sites except Owings have a nearly unobstructed 2π-sr field of view (FOV) of the clear sky; the fisheye images in Figs. 2 and 3 show the USNA site's view of the sky. Table 1 provides other site details. Our spectroradiometers were two Photo Research models PR-650 with wavelength ranges of 380–780 nm and a spectral step size of 4 nm.[20]

Because the ordinary purple light can be found at and near the zenith, we sometimes measured horizontal irradiances with a cosine receptor. More often, however, we measured skylight radiances by aiming the PR-650 spectroradiometer's 1°-FOV telescope at the solar azimuth (relative azimuth, $\phi_{rel} = 0°$) and elevation angle $h = 20°$. This choice of h is arbitrary, but it does agree with existing definitions

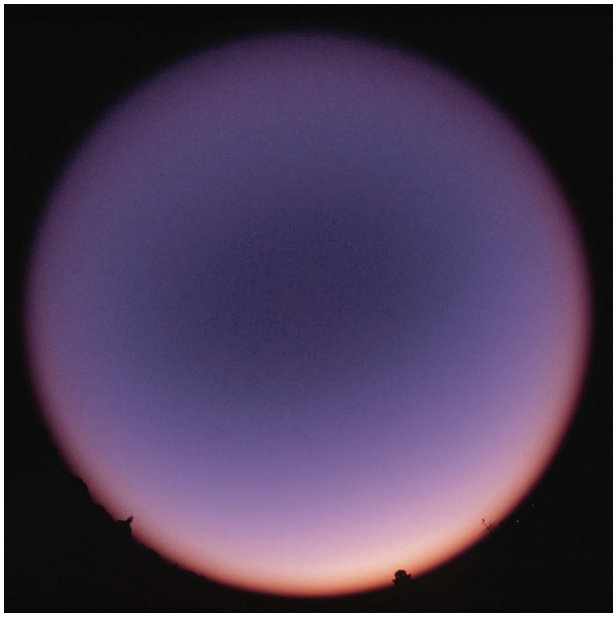

Fig. 2. Fisheye photograph of an ordinary purple light taken during evening twilight at the USNA in Annapolis, Maryland, on 6 October 1997 at 2257 UTC. Solar elevation, $h_0 = -4.07°$; the photograph is centered on the zenith.

of the purple light's location. Using Rozenberg's definition of twilight,[21] we measured skylight spectra at 30-s intervals when $h_0 \leq +5°$. Depending on the value of h_0, we could acquire each visible-wavelength spectrum in 0.02–6 s.

Fig. 3. Fisheye photograph taken during evening twilight at the USNA on 2 October 1997 at 2302 UTC. Solar elevation, $h_0 = -3.85°$; the photograph is centered on the zenith. In contrast to Fig. 2's twilight, this sky has no discernible purple light. Figures 1–3 were all photographed with the same type of color slide film, Kodak Elite II (ISO 100). Exposure times in Figs. 1–3 ranged from 0.008 to 0.5 s, so reciprocity failure and its possible color shifts are unlikely here.

Table 1. Geographic Details of Our Measurement Sites

Site Name	Latitude	Longitude	Elevation (m)
Granada, Spain	37° 11′N	3° 35′W	680
Marion Center, Pa.	40° 49′N	79° 5′W	451
Owings, Md.	38° 41′N	76° 35′W	15
USNA, Md.	38° 59′N	76° 29′W	18

Figure 4 illustrates the purple light's basic scattering geometry. In it, we cut through the Earth to display a cross section of an atmosphere with greatly exaggerated thickness (in reality, the stratosphere extends from altitudes of approximately 10–17 km at the tropopause to ~50 km at the stratopause). Parallel rays of sunlight a–d illuminate a radiometer's or our own line of sight (LOS) from space down to point t above the surface observing site s; Fig. 4 does not show these rays' refraction. Note that the exaggerated atmospheric thickness in Fig. 4 introduces a minor artifact: Unlike in the real atmosphere, none of Fig. 4's tropospheric rays reenter the stratosphere before they reach our LOS. Naturally, radiances received at the surface are the result of extinction losses and scattering gains all along the given LOS.

In Fig. 5 we plot two typical chromaticity curves that result from our time-series spectra of ordinary, or non-volcanic, evening twilights. Although we use the perceptually isotropic CIE 1976 uniform-chromaticity-scale (UCS) diagram, ordinate and abscissa scales differ in Fig. 5 and subsequent chromaticity diagrams in order to show as much detail as possible.[22] Line markers such as the ×'s or small circles in Fig. 5 and other figures distinguish the chromaticity curves from one another but, unless indicated, have no other significance. Some useful colorimetric landmarks in Fig. 5 are the curved

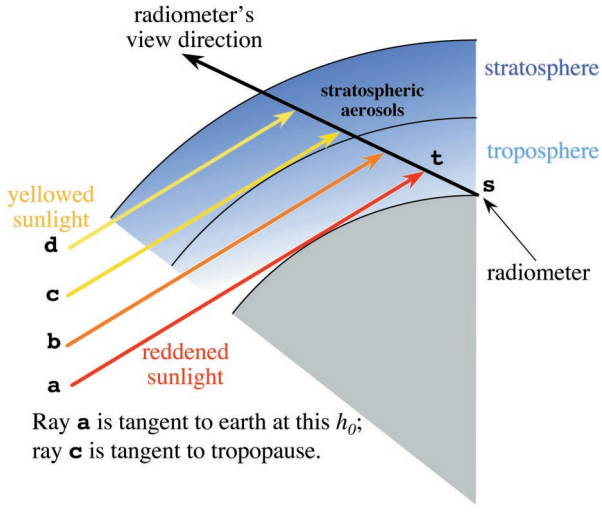

Fig. 4. Simplified scattering geometry for the purple light; atmospheric thickness and Sun elevation are exaggerated here. Before they reach the radiometer's line of sight, parallel rays of sunlight are reddened to varying degrees by transmission through the troposphere or stratosphere.

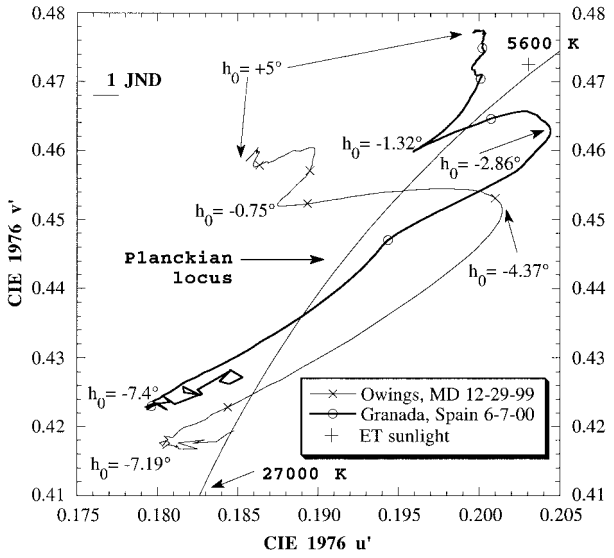

Fig. 5. Portion of the CIE 1976 UCS diagram, showing temporal trends in purple-light chromaticities measured during evening twilights at Owings, Maryland (29 December 1999), and Granada, Spain (7 June 2000). Each spectroradiometer's FOV is 1°, and throughout these measurements its view elevation is $h = 20°$ and its relative azimuth is $\phi_{rel} = 0°$. The cross labeled "ET sunlight" is the chromaticity of sunlight measured above the atmosphere.

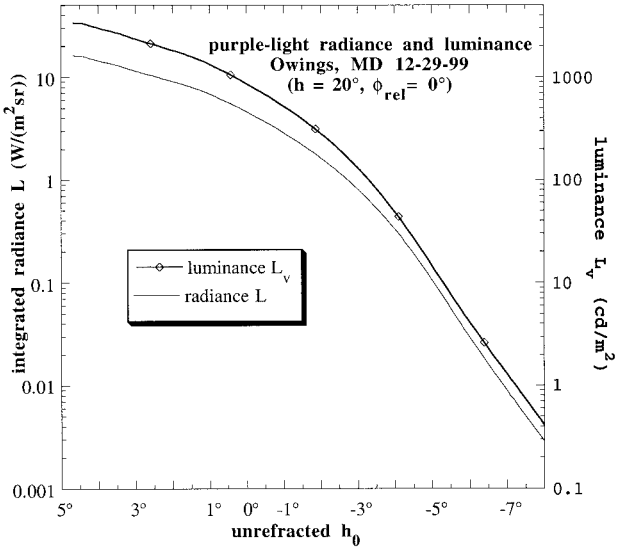

Fig. 6. Purple-light luminance and integrated radiance as functions of h_0 for the 29 December 1999 Owings evening twilight whose chromaticities are shown in Fig. 5.

Planckian locus, two color temperatures, the color of extraterrestrial sunlight above the atmosphere (denoted "ET sunlight"), and a horizontal line labeled "1 JND." This last is a perceptual ruler whose length is the mean MacAdam just-noticeable difference (JND) along our chromaticity curves.[23] Throughout this paper, the scales of JND lines are those of the accompanying u' axis.

The fairly vivid Owings purple light of 12-29-99 begins at local sunset ($h_0 = -0.75°$) as a sharp reversal of the trend that makes skylight increasingly blue for $h_0 < +1.18°$. These purple-light chromaticities cross the Planckian locus en route to maximum vividness (i.e., maximum colorimetric purity) at $h_0 = -4.37°$ and then recross it soon after civil twilight's end ($h_0 \sim -6°$). In fact, this pattern typifies the evolution of a vivid ordinary purple light: (1) as the Sun nears the astronomical horizon, skylight tens of degrees above the horizon reddens until $h_0 \sim 1°$–2°; then (2) this skylight gets bluer until sunset or a few minutes thereafter (<5 min), followed immediately by (3) the start of a purple light whose (4) purity maximum occurs at $h_0 \sim -3.9°$ (see Table 1) and ended by (5) skylight's rapid bluing through the end of evening civil twilight.

Now we must reconsider the term "purity." In our observations the *apparent* purity maximum for any given purple light occurs when its post-sunset chromaticities reach their maximum CIE 1976 u' (or 1931 x) value. In other words, the best purples are seen at the post-sunset "nose," or rightward-most excursion of the chromaticity curve. We define this extreme point on a twilight chromaticity curve as its *purple-light maximum*. During the 12-29-99 Owings twilight, this occurred at $h_0 = -4.37°$, and it is marked with an arrow in Fig. 5. Even though the corresponding u', v' chromaticity is closer than others to such nominal achromatic points as Fig. 5's ET sunlight, the maximum u' chromaticity is consistently the purple light's most visually striking color. One can easily (and legitimately) reconcile observation and colorimetric terminology simply by picking another achromatic point (e.g., use $u' = 0.19$ and $v' = 0.44$ in Fig. 5). The chromaticity of this perceived achromatic stimulus itself depends on surround colors or on those of the ambient illumination (i.e., horizontal irradiances). Given the large, slowly evolving color changes that occur in twilight's ambient illumination, local chromaticity extrema such as Fig. 5's purple-light maxima are easy to interpret as fairly saturated colors, whatever their absolute chromaticities. This apparent conundrum about colorimetric purity demonstrates that, within reasonable limits, the temporal chromaticity curve's *shape* matters more than chromaticity values per se in determining whether a particular purple light is visually impressive.

As noted above, the purple light's increasing saturation is easy to misinterpret as increasing brightness. Figure 6 shows that both purple-light luminance L_v and integrated radiance L indeed decrease steadily with h_0. Figure 5's chromaticity curve reverses once again at $h_0 = -7.19°$, presumably marking the start of the second purple light.[24] The chromaticity curve's erratic wiggles here are instructive: The weak (and thus noisy) signal of the ordinary second purple light is barely detectable by instrument and certainly not by naked eye. At this h_0, skylight's mesopic-level luminances ($\sim$1 cd/m^2) made color vision difficult and chromaticity moot: The sky simply looked dark to us.

At maximum purity, Fig. 5's Granada late-spring

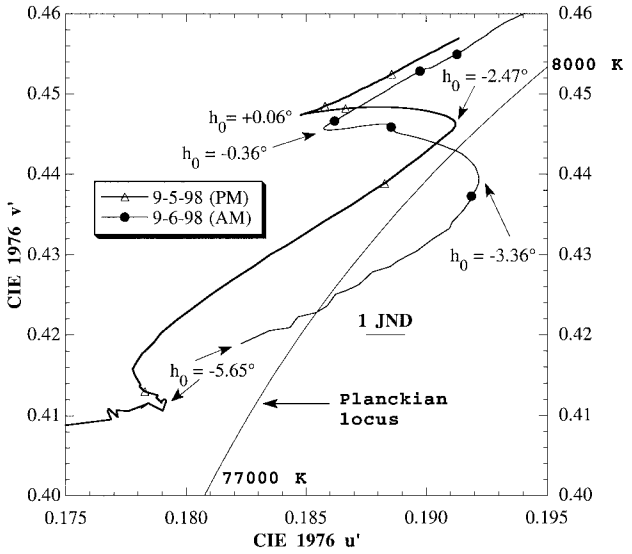

Fig. 7. Temporal trends in purple-light chromaticities measured during adjacent evening (5 September 1998) and morning (6 September 1998) twilights at a rural site near Marion Center, Pennsylvania. Unlike those in Fig. 5, these chromaticities are derived from horizontal irradiances.

purple light is perceptibly redder than its early-winter counterpart. Although Fig. 5 does not gainsay Neuberger's essentially correct statement that the purple light occurs less often in spring than in autumn,[12] it does show that spring purple lights are no less vivid. Equally interesting is the Granada chromaticity cusp at $h_0 = -1.32°$ that marks the purple light's start. Unlike chromaticity cusps observed in angular scans along sky meridians[22] or across the rainbow,[25] these sudden color reversals in the purple light are not accompanied by any abrupt change in radiance. To the naked-eye observer, twilight's slow progress means that such temporal stationary points in sky color go unseen. We examine the physical reason for such chromaticity cusps in Section 6 below.

4. Varietal Purple Lights

The ordinary purple light often dominates the color of ambient illumination during twilight, and so its colorimetric signature not surprisingly appears in chromaticities derived from horizontal irradiances (Fig. 7). Except for their displacement toward the blue, Fig. 7's temporal chromaticity curves from Marion Center look quite similar to their radiance-based counterparts in Fig. 5. However, there are some important differences.

First, the 9-5-98 curve shows no hint of a second purple light. In other words, on this date daylight shows no consistent reddening early in evening nautical twilight. This makes sense because low irradiance levels stopped our measurements at $h_0 = -6.82°$, slightly before the second purple light begins on most evenings (on average, at $h_0 \sim -7.4°$; see Table 2). Furthermore, the single-scattering geometry of nautical twilight means that, unlike the main

Table 2. Summary Statistics for Purple-Light Geometry, 12-29-99 to 11-15-01[a]

Parameter	h_0 (°) Start	Peak	End	Gamut ($\hat{g}$)
Minimum	−3.33	−4.69	−8.46	0.03229
Maximum	−0.22	−1.43	−5.54	0.08645
Mean	−1.411	−3.893	−7.369	0.05249
Median	−1.16	−4.15	−7.4	0.04918
Standard deviation	0.927	0.709	0.559	0.01247

[a]These statistics were calculated over 35 evening purple lights with a colorimetrically distinct start, peak (i.e., maximum purity), and end; spectral radiances were measured at $h = 20°$ and $\phi_{rel} = 0°$. Normalized chromaticity gamut $\hat{g}$ is defined in Ref. 22 and is a measure of the fraction of the CIE 1976 UCS diagram that a chromaticity curve spans.

purple light, the second purple light is confined to the near-horizon sky and thus cannot dominate horizontal irradiances. Of course, during ordinary twilights the near-horizon sky lacks any vivid color at such small h_0.[26] Second, our analyses show that during clear civil twilights approximately 35%–40% of the horizontal irradiance at the surface comes from skylight radiances at $h \geq 45°$, with the result that horizontal irradiances' chromaticities are strongly influenced by these high-h radiances. During evening twilight, the sky becomes purplish sooner at higher h because, at any given moment, a fixed sunlit altitude (say, the tropopause) has a local Sun elevation that decreases as we look toward higher h. So, as twilight progresses, reddened sunlight illuminates the lower stratosphere sooner at higher h, and we first see the purple light there. Because Fig. 7's purple lights are influenced by skylight coming from high h, they start before the purple lights of Fig. 5. Finally, even though Fig. 7's twilights are separated only by ~10 h, notice that their chromaticity curves differ by >1 JND at most h_0. Such dusk-to-dawn variability must be considered as we model the ordinary purple light.

Figure 8 demonstrates that the zenith sky itself can be purplish. Here we measure spectral radiances within a 1° FOV centered on the zenith, a direction where existing accounts disallow the purple light. Even at its most vivid (on 1-21-01), this zenith purple light has a differently shaped chromaticity curve than its low-h kin. As expected, the zenith curves are mostly bluer than those shown in Fig. 5. However, the characteristic purple-light excursion across the Planckian locus remains on 1-21-01, and our color notes judged this zenith sky to be "distinctly purplish" when $h_0 = -3°$. Yet a mere two days later, on 1-23-01, the Owings chromaticity curve is entirely to the left of the Planckian locus and the zenith sky looked only blue.

At this point, readers accustomed to colorimetric absolutism may be reeling. How can we move chromaticity curves around the CIE color space, all the while using the single color adjective "purplish" to describe them? In fact, our colorimetric relativism

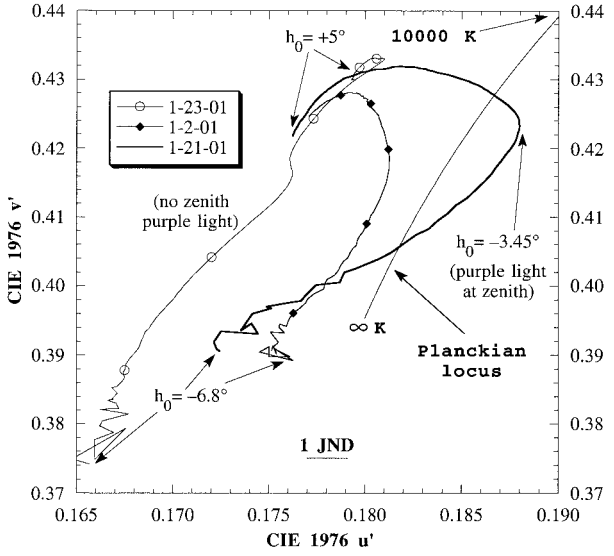

Fig. 8. Temporal trends in evening twilight chromaticities measured at the zenith at Owings, Maryland, on 2, 21, and 23 January 2001. Although the 21 January twilight has a distinct purple light, two days later there is none.

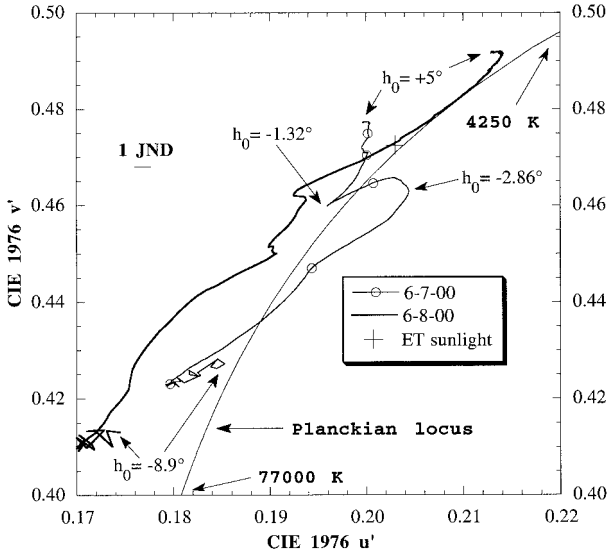

Fig. 10. Comparison of temporal trends in evening twilight chromaticities at Granada on 7–8 June 2000 ($h = 20°$, $\phi_{rel} = 0°$). Note that the vivid purple light of 7 June largely disappears by the next day.

is just a practical example of color constancy: Even though in principle our measured chromaticity curves differ perceptibly from day to day, we judge color in its immediate spatial and temporal context. As noted above, the chromaticity curve's shape tends to be more significant visually than its actual chromaticities. Thus different twilight chromaticities on different days all can look purplish.

How does a given twilight's purple light change with h? Figure 9 answers this question for the evening of 6-7-00 at Granada. To create Fig. 9 we simultaneously measured 1°-FOV radiances at h = 20°, 45° with our two PR-650 spectroradiometers and horizontal irradiances with a third spectroradiometer, a LI-COR model LI-1800.[27] Figure 9's most striking feature is the close similarity between the curves from horizontal irradiances and from radiances at h = 45° (the former curve ends at h_0 = −3.36° because of the LI-1800 instrument's lower sensitivity). This similarity reinforces our remark about Fig. 7 that chromaticities at high h influence the color of horizontal irradiances (i.e., the ambient color of twilight). And, although Fig. 9's h = 20° curve is much redder than the other two, all three kinds of skylight undergo similar changes in color during twilight. This makes good physical sense, because all skylight derives from a similar sequence of color changes undergone by the setting Sun as it illuminates different altitudes in the atmosphere.

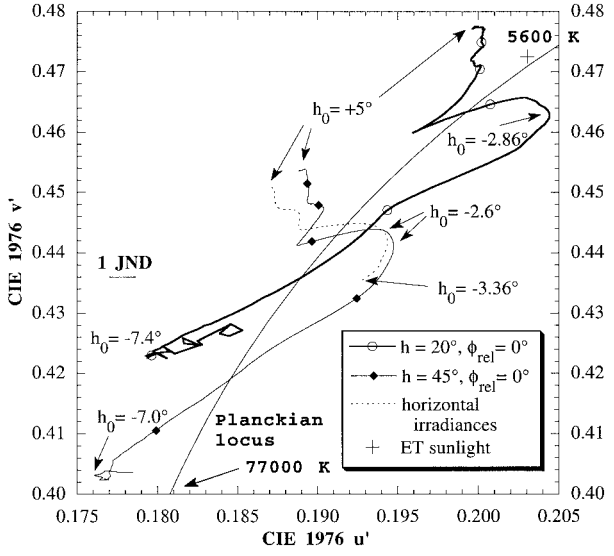

Fig. 9. Temporal trends in evening purple-light chromaticities at Granada, Spain, on 7 June 2000 for horizontal daylight irradiances and for skylight radiances at h = 20°, 45° and ϕ_{rel} = 0°.

Whatever the value of h, marked day-to-day variability is the norm for the ordinary purple light. In Fig. 10, two twilight chromaticity curves pair the vivid Granada purple light of 6-7-00 with a nearly invisible one on 6-8-00 (the 6-7-00 curve also appears in Figs. 5 and 9). Even though both days were cloudless, visibility was distinctly better and atmospheric turbidity lower on 6-8-00. Thus one visual harbinger of a pronounced purple light may be a daytime zenith sky whose blue looks more desaturated than normal.[11] As a corollary, any twilight chromaticity curve with a cusp near sunset or sunrise may indicate the presence of subvisual cirrus (see Section 6 below).

Figure 11 shows just how variable the purple light is, even when it is visible. In Fig. 11 we plot with ×'s the chromaticities of the most vivid purples in 35 different twilights with visible purple lights. Collectively, the chromaticities of these apparently purplish twilights straddle the Planckian locus and have a root-mean-square colorimetric gamut g = 0.01371,[22] or ~8.1 MacAdam JNDs at this u', v'.

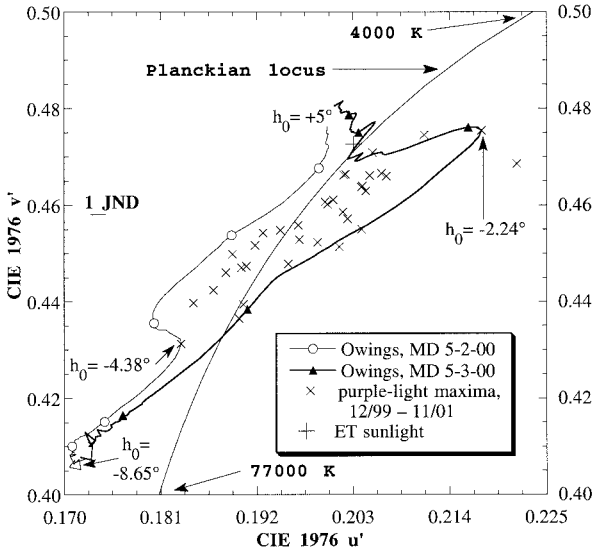

Fig. 11. Variability of 35 purple-light maxima at three of our observing sites. Complete temporal chromaticity curves are drawn for Owings, Maryland, on 2–3 May 2000, two adjacent days with the largest colorimetric difference in purple-light maxima measured from December 1999 to November 2001.

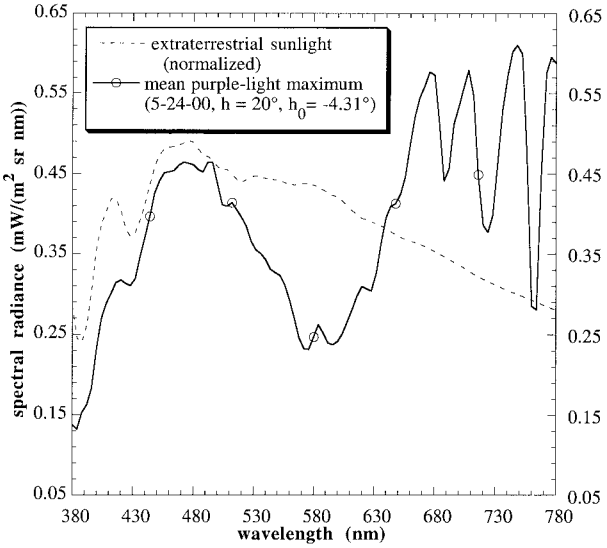

Fig. 12. Visible-wavelength spectral radiances for a typical purple-light maximum measured at Owings on 24 May 2000 when $h_0 = -4.31°$ compared with those of sunlight above the atmosphere (normalized to have the same sum as the purple-light spectrum). Of the 35 purple-light maxima plotted in Fig. 11, this purple-light spectrum has the chromaticity that is closest to the mean u', v'.

We draw chromaticity curves for our two extreme purple-light cases, 5-2-00 and 5-3-00.[28] Although in one day the purple-light maximum underwent the greatest colorimetric shift that we measured in nearly two years, visually this distinct color shift did not seem unusual. Thus Fig. 11 illustrates a fundamental truism about the ordinary purple light: However visually impressive a given purple light is, spectrally based colorimetry may reveal a quite different twilight from the one that you think you saw.

What do purple-light spectra themselves look like? Most resemble the maximum-purity example shown in Fig. 12, measured at Owings on 5-24-00 when $h_0 = -4.31°$. Colorimetrically speaking, this is a proper purple rather than some exotic metamer: Compared with the spectrum of sunlight above the atmosphere, the purple-light spectrum has less energy in the yellows and yellow-greens than in the reds, oranges, and blues. The colorimetric variability seen in Fig. 11 arises largely from shifting balances between Fig. 12's two broad peaks near its spectral extremes, and there are also daily fluctuations in the details of atmospheric absorption bands at wavelengths of >660 nm.

5. The Troposphere's Role in Causing the Purple Light

Figure 11 poses a problem for explanations of the ordinary purple light that rely heavily on the stratosphere. Although we cannot rule out a large 24-h increase in stratospheric aerosol from 2 to 3 May 2000, this seems an improbable first solution. Because Fig. 11's chromaticity extremes occur within 24 h and because there is no record of extreme changes in the stratosphere during that time, the troposphere emerges as a likelier source of this sudden shift in twilight color.

In fact, data from the HALogen Occultation Experiment (HALOE) limb-sounding satellite[29] show that both the differential profiles and the total column amounts of stratospheric aerosols at our site can be *greater* when there is no purple light. Just the opposite would hold true if stratospheric scattering were the sole (or even the chief) factor in causing vivid ordinary purple lights. For example, Fig. 13 shows temporal chromaticity curves for three different twilights. Although the USNA 11-12-98 twilight

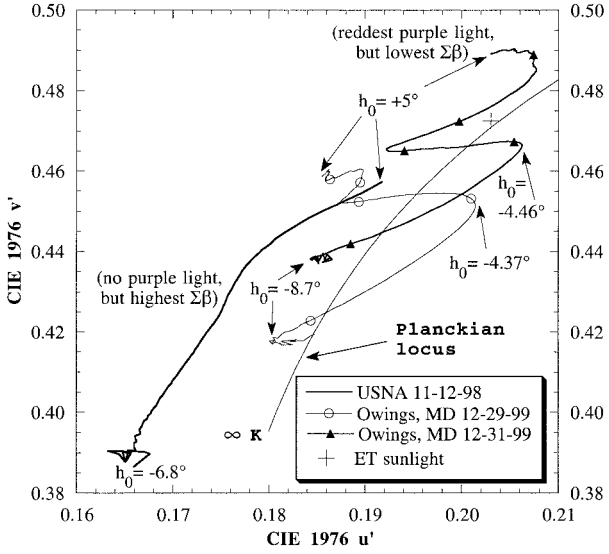

Fig. 13. Temporal trends in evening twilight chromaticities at the USNA (12 November 1998) and at Owings (29 and 31 December 1999). Σβ is the total column amount of stratospheric aerosol measured above these sites (see Fig. 14 for details).

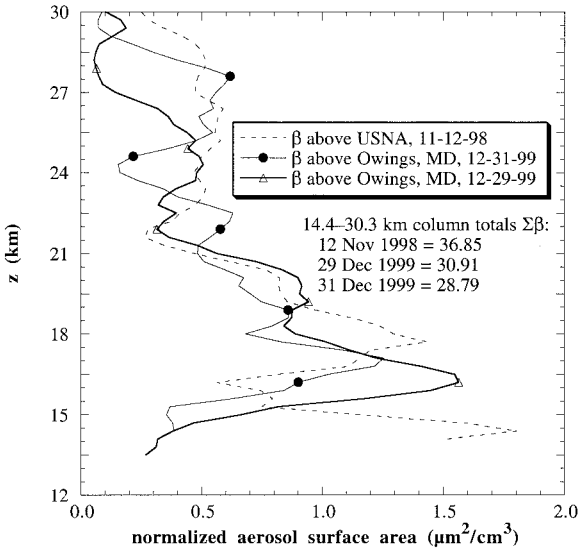

Fig. 14. HALOE limb-sounding satellite measurements of the vertical distribution of normalized aerosol surface area β (square micrometers per cubic centimeter) in the stratosphere, interpolated to the latitudes and longitudes of the USNA (on 12 November 1998) and of Owings (on 29 and 31 December 1999). Compare the total column amounts Σβ of these scatterers with twilight colors on the same dates in Fig. 13.

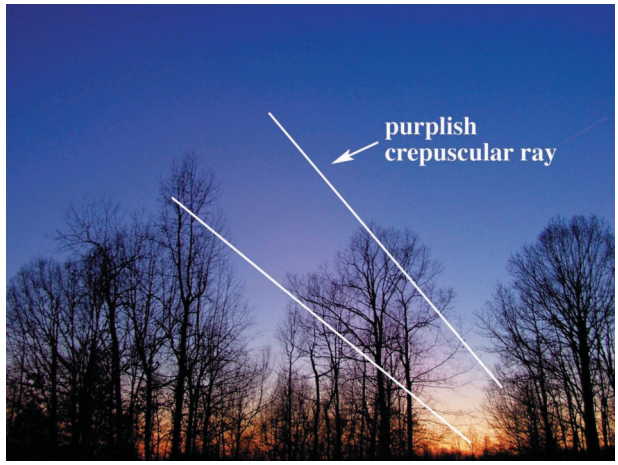

Fig. 15. Photograph of a purplish twilight crepuscular ray at Owings on 1 January 2002 at 2222 UTC ($h_0 = -5.43°$). White lines have been drawn on the sky to help to locate this low-contrast ray.

has no purple light, the Owings 12-29-99 purple light (see Fig. 5 for a closer view) is vivid but clearly less red than that on 12-31-99.

Now compare these chromaticity curves with Fig. 14's HALOE vertical profiles of stratospheric aerosols on the same dates. These aerosols are primarily sulfuric acid droplets, and their median radii are smaller than 0.1 μm at all altitudes z. Summing these droplets' normalized surface areas β (in square micrometers per cubic centimeter) for z from 14.4 to 30.3 km (Ref. 30) reveals that 11-12-98 has the largest column total Σβ and 12-31-99 has the smallest Σβ. This result is opposite that expected if stratospheric aerosol concentration alone determined the vividness (or even the existence) of the ordinary purple light. Nor does the vertical distribution $\beta(z)$ solve this conundrum: When the 12-31-99 purple light is at its purest ($h_0 \sim -4.46°$), all sunlight rays that pass through the troposphere en route to our radiometer's LOS intersect that line at $z < 21$ km. These rays pass beneath tropopause-grazing ray c in Fig. 4. Yet $\beta(z)$ below 21 km usually is smaller on 12-31-99 than on Fig. 13's other two dates. So neither the vertical distribution nor the column totals of stratospheric aerosols can by themselves account for its purple lights.

Because spectrally selective extinction is much greater in the troposphere than in the stratosphere, the troposphere provides the reddest illumination of stratospheric aerosols along our LOS. (We support this claim quantitatively in Section 6 below). If the stratosphere does not predominate in creating ordinary twilights' colors, then the troposphere must. Figures 13 and 14 provide indirect evidence of the troposphere's importance in influencing twilight colors, including the purple light. Direct visual evidence comes from Fig. 15's twilight crepuscular ray. Often noted by purple-light observers,[31] these low-contrast rays can span the entire sky as alternating bands of pinkish-purple and blue: i.e., the purple light flanked by its absence. Shadows cast on the lower stratosphere eliminate the purple light within the blue bands, and mountains and tropospheric clouds far beyond the sunset horizon usually cast these shadows. Thus the purple light disappears if the stratosphere above us is shaded from sunlight that has been reddened by transmission through the troposphere.

We can best explain Fig. 13's variable purple light by examining Fig. 16. Each of these geostationary satellite images was taken within a few hours of our corresponding twilight measurements in Fig. 13. In each part of Fig. 16 we have drawn a red arrow from our observing site toward the Sun's azimuth when $h_0 = -4.5°$, i.e., toward the Sun when the purple light is near its peak. The arrow's tip marks the point where the Sun's unrefracted rays would then be tangent to the Earth's surface. Notice that only for the two December 1999 twilights does a long cloud-free path extend from our site toward sunset. On those days, tropospherically reddened sunlight can illuminate the lower stratosphere along our LOS, and thus the purple light forms. But on 11-12-98 [Fig. 16(c)] a large cirrus shield to our southwest prevented direct sunlight from being transmitted along long slant paths through the troposphere to our LOS. Although sunlight that has been slightly yellowed by transmission through the stratosphere illuminates our radiometer's LOS, no tropospherically reddened sunlight reaches it. As a result, no purple light formed on 11-12-98. In our research, this cause-and-effect relationship between the purple light and clouds far over the sunset–sunrise horizon is quite consistent: Every clear twilight without a purple light has some cloud cover in

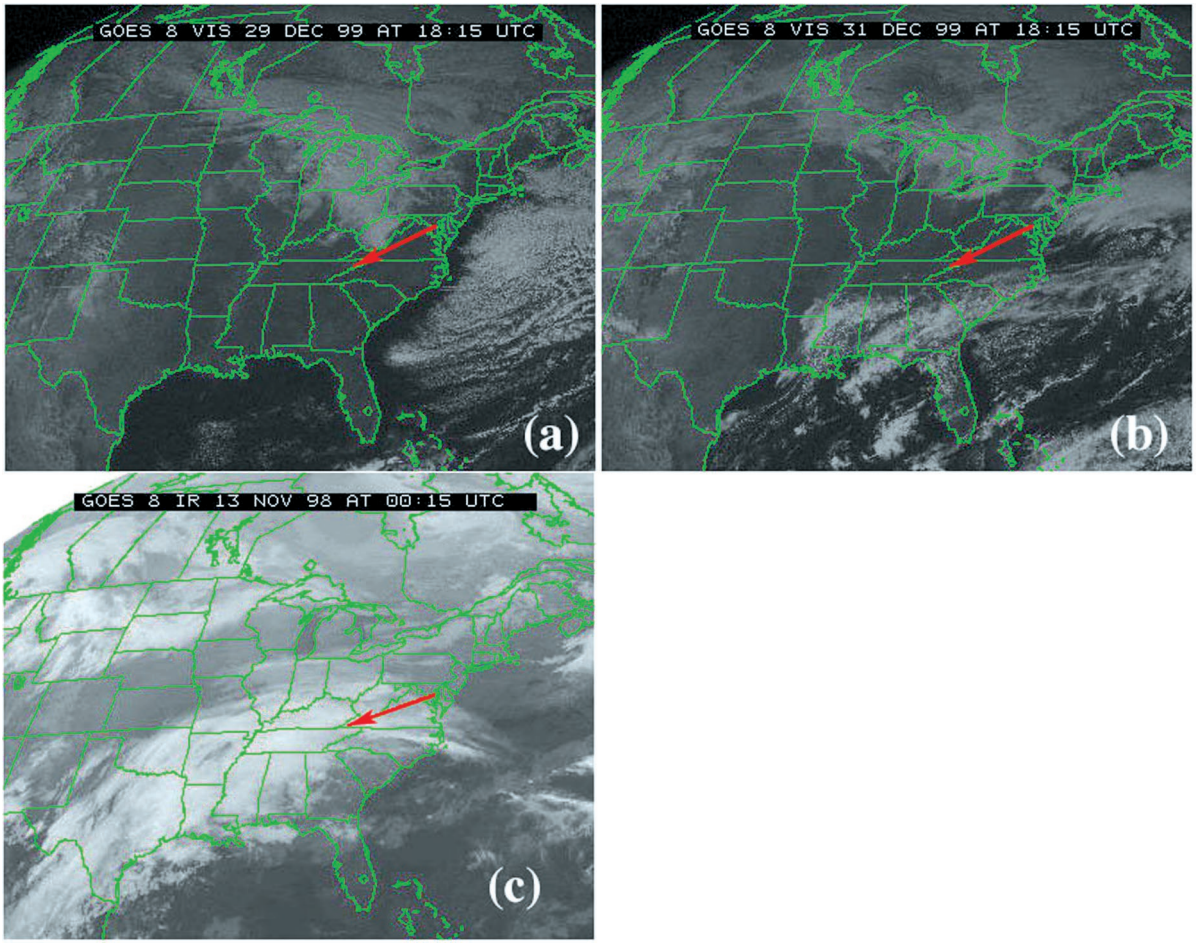

Fig. 16. Visible- and infrared-wavelength geostationary satellite images of the United States (a), (b) on the afternoons of 29 December 1999 (visible wavelengths) and 31 December 1999 (visible), respectively, and (c) in the early evening of 12 November 1998 (infrared). Red arrows point from our observing sites toward the Sun's azimuth at $h_0 = -4.5°$. Clouds far beyond our sunset horizon on 12 November eliminated the purple light then (see Fig. 13).

the Sun's direction. This cloud cover need not be extensive and may be hundreds of kilometers distant, but it is always present.

In fairness, Bullrich states explicitly[16] and Deirmendjian implies[10] that distant clouds matter in explaining the purple light. But, until now, the purple light's disappearance usually has been regarded as little more than a matter of *local* cloud climatology.[12] In fact, a thin to moderately thick overcast does not rule out the purple light's formation. Although one cannot see the clear sky through an overcast, our measurements show that the purple light's diffuse illumination above the clouds makes some overcast twilights (briefly) at least as purple as their clear-sky counterparts. Yet whether the day is clear or cloudy, the purple light disappears if clouds anywhere along the Sun's azimuth prevent tropospherically reddened sunlight from illuminating the stratosphere above us.

6. Modeling the Purple Light

To dissect the purple light's complexities, we turn to LOWTRAN 7, a radiative-transfer model that incorporates considerable meteorological detail.[32,33] To make realistic comparisons with Fig. 13's measurements of ordinary purple lights, our LOWTRAN simulations in Fig. 17 include the following parameters: a default midlatitude winter atmospheric profile of temperature, pressure, humidity, and gas mixing ratios; tropospheric aerosols typical of rural sites; background stratospheric dust and other aerosols (i.e., ordinary rather than volcanic twilights); no clouds or rain; multiple scattering; a surface albedo of 0.2; and Mie aerosol phase functions. Consistent with our measurements of radiance spectra, the model is set to calculate skylight spectral radiances at $h = 20°$, $\phi_{rel} = 0°$.

Keeping these parameters constant in Fig. 17, we vary h_0 and horizontal meteorological range V.[34] As tropospheric turbidity and mean extinction coefficient increase, V decreases and sunsets tend to become redder. A corollary result is that, as V decreases, irradiances illuminating stratospheric scatterers along our LOS during twilight are redder at a given h_0. Our reference case in Fig. 17 sets $V =$ 23 km, a value that is typical of clear rural atmospheres. All the features seen in Fig. 13 are reproduced in this case: (1) pre-sunset reddening is followed by rapid bluing of skylight before sunset; (2)

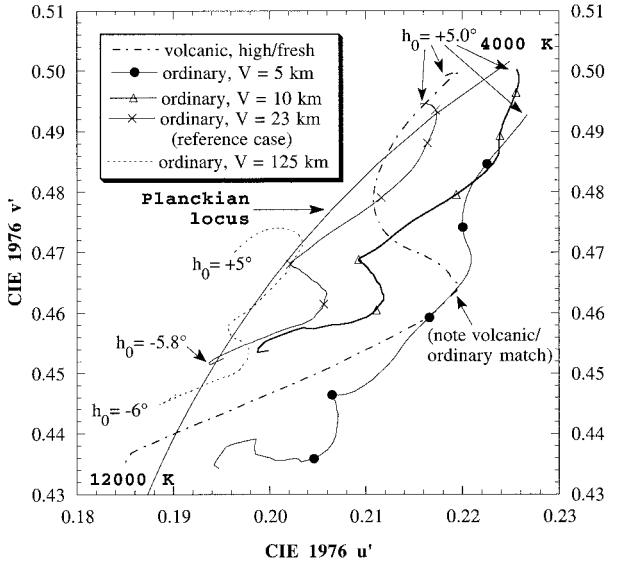

Fig. 17. Radiative transfer model LOWTRAN 7's calculations of temporal chromaticity trends for ordinary purple light as functions of h_0 and meteorological range V at $h = 20°$ and $\phi_{rel} = 0°$. For comparison, we also show a chromaticity curve calculated for a volcanic twilight with high levels of fresh volcanic scatterers in the stratosphere. Note the similarities between the $V = 23$ km curve (our LOWTRAN reference case) and the purple-light chromaticities measured in Figs. 5 and 13.

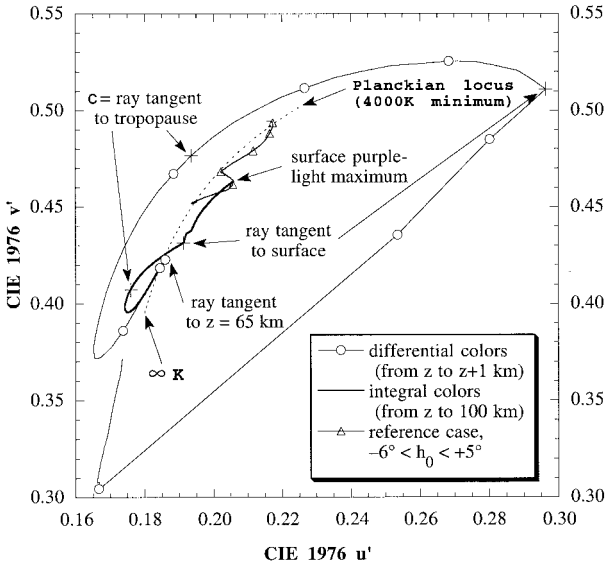

Fig. 18. Differential and path-integrated skylight colors predicted by LOWTRAN 7 for Fig. 17's reference case at $h_0 = -4°$ and along the line of sight $h = 20°$ and $\phi_{rel} = 0°$. In this figure only, the pluses at which the arrows point denote particular tangent-ray altitudes. For comparison, we also show the entire surface-based twilight curve for the reference case shown in Fig. 17.

the purple light starts shortly after sunset; (3) reaches its maximum at $h_0 = -4°$, and (4) is followed by a second purple light that begins near civil twilight's end. Decreasing V makes the purple light redder and more vivid and expands its gamut (see the $V = 5$, 10 km curves), whereas increasing V does the opposite ($V = 125$ km curve). Although these results make good physical sense, a less intuitively obvious result is that combining background stratospheric aerosols with a turbid troposphere ($V = 5$ km) yields twilight purples that match the most vivid ones seen in a post-volcanic twilight.

We have claimed that tropospheric extinction produces most of the red component seen in ordinary purple lights (see Fig. 12). Figure 18's LOWTRAN simulation provides strong colorimetric support for this claim. In Fig. 18 we have redrawn the Planckian locus and Fig. 17's reference case at a much smaller scale to show the differential and integral colors predicted as we move down along Fig. 4's LOS for $h_0 = -4°$ (LOWTRAN's purple-light maximum). The strongest source of skylight radiances in our LOS is singly scattered direct sunlight. In turn, this sunlight has been transmitted through various optical thicknesses of the atmosphere to reach our LOS. We calculate skylight's integral colors by summing net skylight radiances along this slant path from the top of the LOWTRAN atmosphere (100 km) down to altitude z km. A similar calculation yields differential colors from z to $z + 1$ km. When $z = 0$ km, the model by definition reproduces the chromaticity that a surface-based observer sees, and so the path-integrated chromaticity curve intersects the reference case's curve (h_0 is not fixed for the latter).

What does Fig. 18 reveal? As we move toward the surface along our LOS, we use as landmarks the tangent (i.e., lowest) heights of sunlight rays that intersect it; the intersections themselves occur at higher altitudes. Beginning with the ray whose refracted tangent height $z = 65$ km, we find initially that differential skylight colors get bluer than is possible by Rayleigh single scattering (whose chromaticity corresponds to infinite color temperature). This enhanced bluing apparently is caused by stratospheric ozone absorption in the spectral Chappuis bands centered near 600 nm.[35] As tangent height z decreases still further, differential contributions to path-integrated sky color reverse near $u' = 0.16$; they next grow greener, and then yellower. Ray c in Fig. 18 has its tangent height at the tropopause ($z = 10$ km in LOWTRAN; Fig. 4), and it is the last stratosphere-only contribution to the path-integrated skylight color that we see at the surface. Rays below c are transmitted though ever-increasing optical thicknesses of the troposphere.

Although the differential contribution of ray c is yellowish-green, path-integrated color at the tropopause along our surface-based LOS looks distinctly blue. Only as we add scattering from sunlight rays that have traversed the troposphere do we get red contributions to surface skylight. Of course, because tropospheric extinction increases rapidly with decreasing altitude, tropospheric rays make ever-redder, but also ever-weaker, additions to the surface signal. Yet, even after scattering from Fig. 18's reddish surface-grazing ray has been added, the integral skylight color has covered only approximately half of

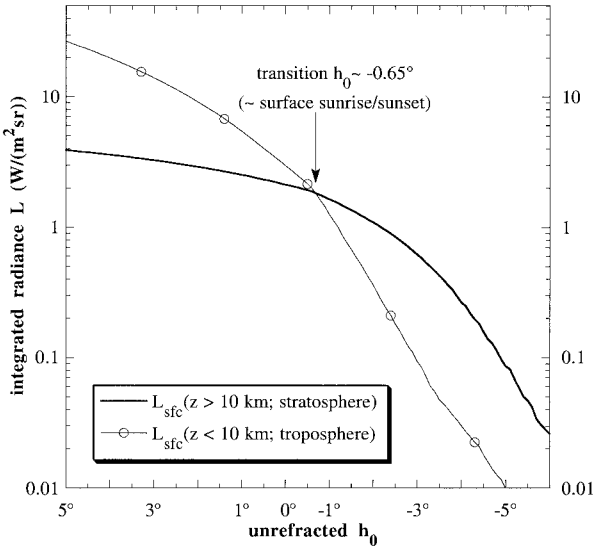

Fig. 19. LOWTRAN 7 calculations of the h_0 dependence of the stratospheric and tropospheric components of skylight radiances received at the Earth's surface. The model atmosphere here is Fig. 17's reference case, and the observer's line of sight is $h = 20°$ and $\phi_{rel} = 0°$.

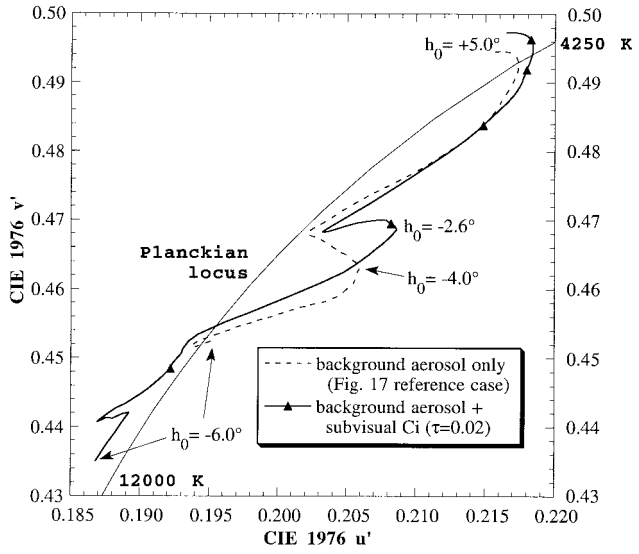

Fig. 20. LOWTRAN 7 calculations of the effects of subvisual cirrus on purple-light chromaticity trends, including the formation of a chromaticity cusp near sunset. The uniform cirrus layer's base is at 10 km, and its normal optical thickness, τ, is 0.02.

the colorimetric distance from ∞K to its final purplish color at our eye. By definition, the remaining radiance that reaches us must come from multiple scattering within the Earth's shadow, and this last differential contribution is purplish to blue (Fig. 18, lower left). The stratosphere is far from irrelevant here, because it provides some of the bluish molecular-scattering contribution seen at Fig. 12's short wavelengths. Yet LOWTRAN indicates that scattering and extinction within the troposphere (including multiple scattering) are by far the most important processes in creating the ordinary purple light's red components.

Finally, what can we tell from LOWTRAN about the chromaticity cusps seen in Figs. 5 and 7? Part of the answer comes in Fig. 19, where we plot as functions of h_0 two parts of the spectrally integrated LOWTRAN radiances received at the surface. We call the part of path-integrated L that originates solely in the troposphere $L_{sfc}(z < 10$ km). The other part is $L_{sfc}(z > 10$ km), and it originates in the stratosphere; its Fig. 19 values reflect extinction losses *after* transmission through the troposphere to the surface. Thus Fig. 19 tells a simple story: At $h_0 \sim -0.65°$, the stratosphere's contributions to surface radiances first exceed those from the troposphere. At still lower h_0, stratospheric radiances begin to outweigh their tropospheric kin.

Although this result may seem to contradict Fig. 18's arguments, in fact it does not: For Fig. 18 it made sense to discuss *tangent* heights for sunlight rays that intersect our LOS. At $h_0 = -4°$, these tangent heights are much lower than the subsequent LOS *intersection* heights, which is the altitude given in Fig. 19. For example, when $h = 20°$ and $h_0 = -4°$, the point whose $z = 10$ km on our LOS is actually several kilometers within the Earth's geometric shadow (i.e., this point's "tangent height" is negative).

Figure 20 completes the important puzzle of the chromaticity cusps. There we repeat our LOWTRAN reference case's chromaticity curve for the ordinary purple light and label it "background aerosol only." Next we add a 500-m thick veil of subvisual cirrus at $z = 10$ km and make this cloud's normal optical thickness $\tau = 0.02$, a realistically small value. The effect is striking: We redden the start of evening twilight and considerably sharpen the chromaticity corner that marks the purple light's onset. If we double τ to 0.04 (not shown), this corner changes to a dagger-sharp cusp, a likely colorimetric signature for subvisual cirrus. Why does this sudden transition occur? We infer from Fig. 19 that stratospheric and tropospheric contributions to surface skylight are approximately equal at sunset. Now we have added a thin layer of cirrus at the tropopause. Although this layer's Sun elevation is slightly higher than that at the surface, its forward scattering of reddened, grazing-incidence sunlight nonetheless increases sharply close to the time of surface sunset. We measure the net result as an unusually sharp reversal of skylight's pre-sunset color trend—and as an abrupt start of the purple light. Thus, although the ordinary purple light may never be a mainstay remote-sensing tool, it continues to present us with an unexpected combination of celestial beauty and optical insight.

7. Conclusions

What simple physical explanation can we offer for the sequences of ordinary twilight colors shown in Figs. 5 and 7? As the Sun sinks below $h_0 = 5°$, rapid increases in slant-path optical thickness for direct sunlight at first redden the irradiances incident on tropospheric scatterers (Fig. 21). Although sunlight

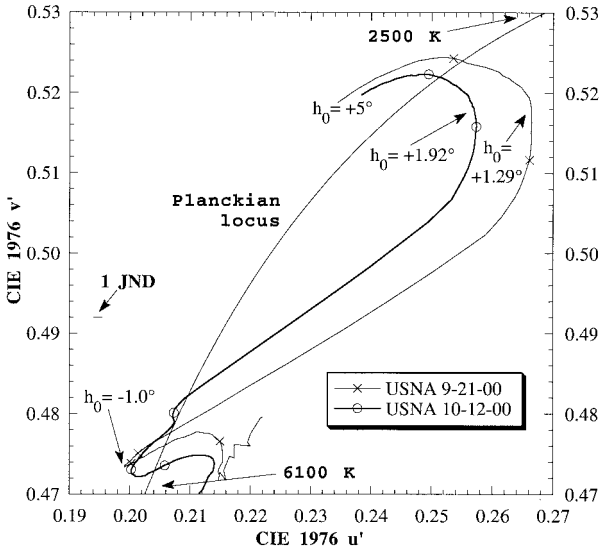

Fig. 21. Temporal trends in the colors of twilight irradiances illuminating a vertical plane that faces the Sun, measured at the USNA on 21 September and 12 October 2000. When $h_0 < 1°–2°$, the irradiance from skylight begins to exceed that from direct sunlight, thus causing scattering by tropospheric scatterers to become increasingly bluish then.

radiances grow ever redder, their rapidly decreasing magnitude means that, when surface $h_0 = 1°–2°$, the incident *irradiance* on these scatterers starts to become bluer (i.e., skylight now begins to dominate this irradiance). Soon after sunset, the still-illuminated stratosphere begins to predominate over a troposphere that is passing rapidly into shadow (Fig. 19), and reddened sunlight sent to the surface by stratospheric scatterers results in the reddening of skylight that marks the purple light's onset.

Although skylight radiances continually decrease during evening twilight, a combination of (1) tropospherically reddened sunlight that is singly scattered in the stratosphere and (2) purplish skylight that is multiply scattered in the troposphere at first increases this skylight's red component. The detailed vertical distribution of stratospheric scatterers (primarily sulfuric acid droplets) appears to be less important in causing this reddening than the simple fact that the scatterers are present. For $h_0 < -4°$, process (1) above fades into insignificance as the lower, denser parts of the stratosphere pass into shadow. Now ozone absorption and molecular single scattering in the stratosphere combine with bluish multiple scattering in the troposphere to make skylight increasingly blue. This process continues until tropospherically reddened sunlight illuminates a stratum of scatterers at even higher altitudes. For nonvolcanic twilights, however, this second purple light has such low luminance that we cannot see either its color or its enhanced brightness.

Thus the ordinary purple light is both simpler and more complex than previously thought: Molecular scattering of sunlight at high altitudes, combined with reddened illumination of the stratosphere and the troposphere, produces the subtle purples of nonvolcanic twilights. LOWTRAN 7 shows that although stratospheric scatterers are needed to send reddened sunlight to the surface, at most they yellow (rather than redden) sunlight transmitted through the stratosphere alone. The resulting purples' details depend largely on daily, or even hourly, changes in the troposphere's optical properties beyond the sunset horizon.

Several agencies generously funded this research. R. L. Lee was supported by National Science Foundation grant ATM-9820729, the U.S. Naval Academy's Departments of Mathematics and Physics, and by the Commander, U.S. Naval Meteorology and Oceanography Command. J. Hernández-Andrés was supported by Spain's Comisión Interministerial de Ciencia y Tecnología under research grant BFM 2000-1473.

References and Notes

1. F. A. R. Russell, "Previous analogous glow phenomena, and corresponding eruptions," in *The Eruption of Krakatoa, and Subsequent Phenomena*, G. J. Symons, ed. (Trübner, London, 1888), pp. 384–405.
2. J. E. Clark, "The remarkable sunsets," Nature **29,** 130–131 (1883).
3. F. A. R. Russell, "Proximate physical cause of the unusual twilight glows in 1883–4," in *The Eruption of Krakatoa, and Subsequent Phenomena*, G. J. Symons, ed. (Trübner, London, 1888), pp. 178–196.
4. A. Riggenbach, *Beobachtungen über die Dämmerung insbesondere über das Purpurlicht und seine Beziehungen zum Bishop'schen Sonnenring* (Georg, Basel, Switzerland, 1886).
5. P. Gruner and H. Kleinert, *Die Dämmerungserscheinungen* (Grand, Hamburg, Germany, 1927), pp. 103–107.
6. A. Heim, "Explanations of the western purple light and the eastern afterglow (Nachglühen)," Mon. Weather Rev. **44,** 624–625 (1916). Although we write "diffraction" here to match the terminology found in Heim's and earlier accounts, nowadays we use both the language and the physics of single-scattering theories such as Mie theory in explaining the purple light.
7. J. V. Dave and C. L. Mateer, "The effect of stratospheric dust on the color of the twilight sky," J. Geophys. Res. **73,** 6897–6913 (1968).
8. F. E. Volz, "Twilights and stratospheric dust before and after the Agung eruption," Appl. Opt. **8,** 2505–2517 (1969).
9. H. H. Lamb, "Volcanic dust in the atmosphere; with a chronology and assessment of its meteorological significance," Phil. Trans. R. Soc. London Ser. A **266,** 425–533 (1970).
10. D. Deirmendjian, "On volcanic and other particulate turbidity anomalies," Adv. Geophys. **16,** 267–296 (1973).
11. G. E. Shaw, "Observations of two stratospheric dust events," J. Appl. Meteorol. **14,** 1619–1620 (1975).
12. H. Neuberger, *Introduction to Physical Meteorology* (Pennsylvania State U. Press, University Park, Pa., 1957), pp. 184–185, 190.
13. J. Walker, *The Flying Circus of Physics with Answers* (Wiley, New York, 1977), p. 274.
14. M. G. J. Minnaert, *Light and Color in the Outdoors* (Springer-Verlag, New York, 1993), pp. 296, 298, 303.
15. D. K. Lynch and W. Livingston, *Color and Light in Nature* (Cambridge U. Press, Cambridge, 1995), p. 41.
16. K. Bullrich, *Die farbigen Dämmerungserscheinungen* (Birkhäuser, Basel, Switzerland, 1982), pp. 69–70.
17. T. Simkin and R. S. Fiske, *Krakatau 1883: The Volcanic*

Eruption and Its Effects (Smithsonian Institution Press, Washington, D.C., 1983), p. 418.
18. T. S. Glickman, ed., *Glossary of Meteorology*, 2nd ed. (American Meteorological Society, Boston, Mass., 2000), p. 605.
19. The period during which we measured twilight spectra had no unusual volcanism, so our data are of ordinary rather than volcanic purple lights. Also, our measurements are confined to evening twilights (with one important exception), and strictly speaking so are our conclusions about the purple light.
20. PR-650 spectroradiometer from Photo Research, Inc., 9731 Topanga Canyon Place, Chatsworth, Calif. 91311. According to Photo Research, at specified radiance levels a properly calibrated PR-650 instrument measures luminance and radiance accurately to within $\pm 4\%$ and has a spectral accuracy of ± 2 nm, and its CIE 1931 colorimetric errors are $x < 0.001$, $y < 0.001$ for a 2856-K blackbody (CIE standard illuminant A).
21. G. V. Rozenberg, *Twilight: A Study in Atmospheric Optics* (Plenum, New York, 1966), p. 17. In purely astronomical terms, civil twilight is the period between sunset or sunrise and $h_0 = -6°$; nautical twilight is the period when $-6° > h_0 > -12°$.
22. For an overview of the entire CIE 1976 UCS diagram, see R. L. Lee, Jr., "Twilight and daytime colors of the clear sky," Appl. Opt. **33,** 4629–4638, 4959 (1994).
23. G. Wyszecki and W. S. Stiles, *Color Science: Concepts and Methods, Quantitative Data and Formulae*, 2nd ed. (Wiley, New York, 1982), pp. 306–310. Here we follow convention and set the JND equal to the semimajor axis length of the MacAdam color-matching ellipse at the given chromaticity.
24. E. L. Deacon, "The second purple light," Nature **178,** 688 (1956).
25. R. L. Lee, Jr. and A. B. Fraser, *The Rainbow Bridge: Rainbows in Art, Myth, and Science* (Pennsylvania State U. Press, University Park, Pa., 2001), pp. 266–267.
26. During some volcanic twilights, the second purple light *is* vividly colored (hence its name) because increased concentrations of liquid aerosols and dust in the stratosphere scatter much more sunlight to the surface.
27. LI-1800 spectroradiometer from LI-COR, Inc., 4421 Superior Street, Lincoln, Neb. 68504-1327. According to LI-COR, at specified radiance levels a properly calibrated LI-1800 instrument measures visible-wavelength spectral radiances accurate to within $\pm 5\%$ and has a spectral accuracy of ± 2 nm, and its CIE 1931 colorimetric errors are $x < 0.003$, $y < 0.003$ for primaries that are typical of a cathode-ray-tube color monitor.
28. The $\times$ to the right of Fig. 11's 5-3-00 purity maximum occurred on 6-11-01. Although this $\times$ is more purplish than the 5-3-00 maximum, the 6-11-01 maximum is actually *closer* to the chromaticity of 5-2-00. Thus the largest chromaticity shift that we measured is from 5-2-00 to 5-3-00, even though Fig. 11's anisotropic scaling suggests otherwise.
29. J. M. Russell III, HALogen Occultation Experiment (HALOE) home page, http://haloedata.larc.nasa.gov/home.html, accessed 7 May 2002.
30. Note that 14.4–30.3 km is the largest altitude range for which HALOE data exist on all three dates in Fig. 14. Meteorological soundings on these dates from nearby Dulles International Airport have temperature inversions that place the local tropopause at altitudes of 12.3–15.7 km.
31. For example, see Ref. 5, Plate 5.
32. R. W. Fenn, S. A. Clough, W. O. Gallery, R. E. Good, F. X. Kneizys, J. D. Mill, L. S. Rothman, E. P. Shettle, and F. E. Volz, "Optical and infrared properties of the atmosphere," in *Handbook of Geophysics and the Space Environment*, A. S. Jursa, ed. (U.S. Air Force Geophysics Laboratory, Hanscom Air Force Base, Bedford, Mass., 1985), pp. 18:1–18:80.
33. F. X. Kneizys, E. P. Shettle, L. W. Abreu, J. H. Chetwynd, G. P. Anderson, W. O. Gallery, J. E. A. Selby, and S. A. Clough, "User's Guide to LOWTRAN 7," Rep. AFGL-TR-88-0177 (U.S. Air Force Geophysics Laboratory, Hanscom Air Force Base, Bedford, Mass., 1988).
34. Ref. 18, p. 488.
35. C. N. Adams, G. N. Plass, and G. W. Kattawar, "The influence of ozone and aerosols on the brightness and color of the twilight sky," J. Atmos. Sci. **31,** 1662–1674 (1974).